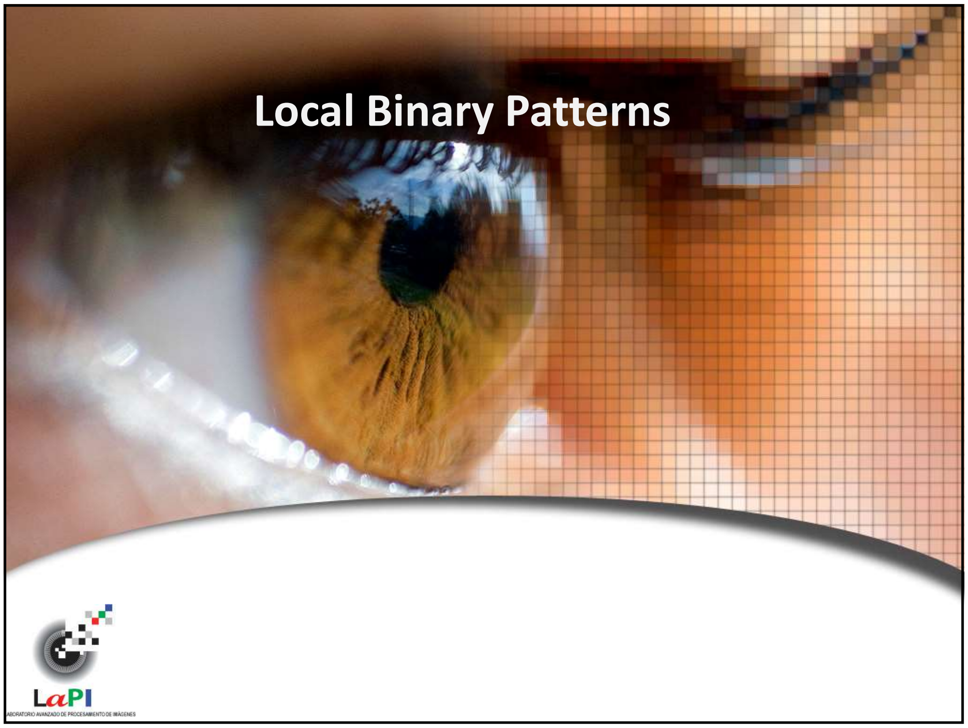

1

Local Binary Patterns [OJALA et al 1996]

•LBPs are operators that transform image ⇨ integer labels

•Labels can be represented as histograms (fingerprints)

•Invariant to rotations and monotonic gray level changes.

•Detection and Classification

•Great variation on real images

•Contrast Distribution

•Different angles of an image, light changes , noise or occlusions

•Texture classification, facial recognizing and object categorization

2

86	102	15
77	83	56
101	95	70

Binary code = 11000110

Decimal value = 128+64+4+2 = 198

3

Local Binary Patterns

$$LBP_{P,R} = \sum_{p=0}^{P-1} s(g_p - g_c)2^p.$$

$$s(x) = \begin{cases} 1, x \geq 0 \\ 0, x < 0. \end{cases}$$

R- radius
P-sampling points
gc- central pixel
gp – neighbor pixels
s - comparison function

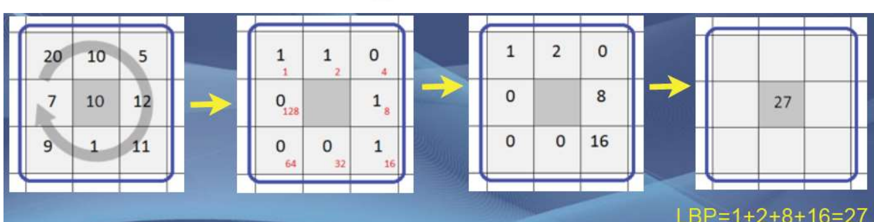

UNAM • TODOS LOS DERECHOS RESERVADOS © MÉXICO, 2011

4

Local Binary Patterns -LBPs

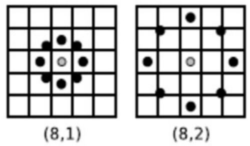

$$LBP_{P,R}\left(g_c\right) = \sum_{p=0}^{P-1} s\left(g_p - g_c\right) 2^p$$

Circular region
R-radius
P-sampling points
g_c*- central pixel*
g_p *– other pixels*
s - comparision function

5

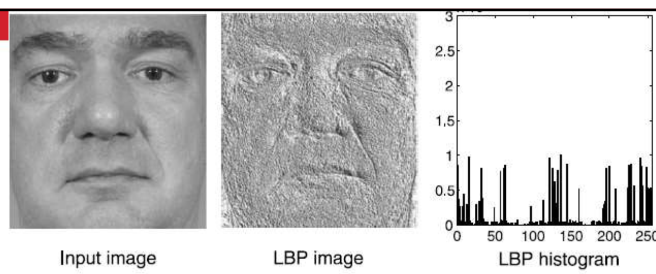

Fig. 2.1 Example of an input image, the corresponding LBP image and histogram

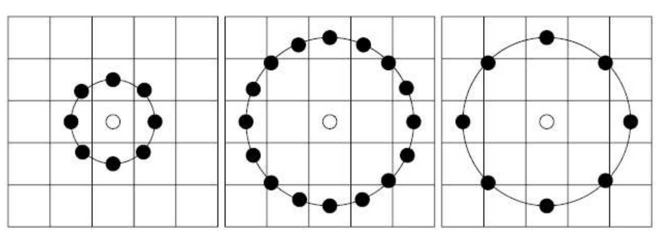

Fig. 2.2 The circular (8, 1), (16, 2) and (8, 2) neighborhoods. The pixel values are bilinearly interpolated whenever the sampling point is not in the center of a pixel

Tomado del libro de Matti_Pietikäinen, Abdenour_Hadid, Guoying_Zhao, Timo_Ahonen. Computer Vision Using Local Binary Patterns 2011

6

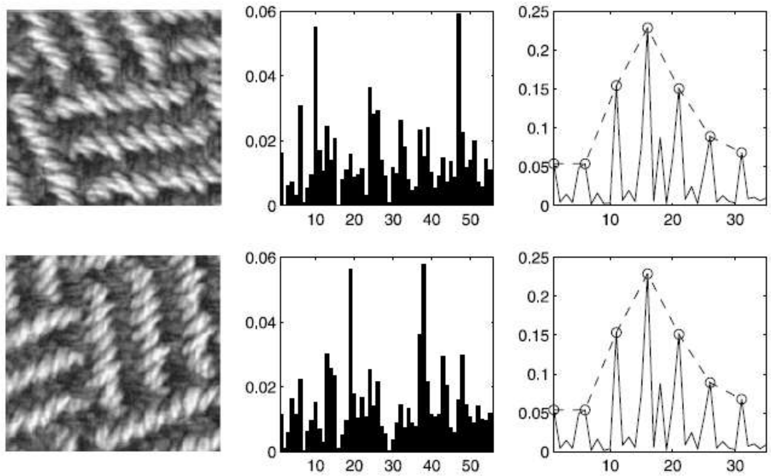

Fig. 2.6 *1st column*: Texture image at orientations 0° and 90°. *2nd column*: bins 1–56 of the corresponding LBP^{u2} histograms. *3rd column*: Rotation invariant features $|H(n,u)|$, $1 \le n \le 7$, $0 \le u \le 5$, (*solid line*) and LBP^{riu2} (*circles, dashed line*). Note that the LBP^{u2} histograms for the two images are markedly different, but the $|H(n,u)|$ features are nearly equal

7

Local Binary Patterns -LBPs

•Uniform LBP

$$LBP_{P,R}^{uni}(g_c) = \begin{cases} \sum_{p=0}^{P-1} s(g_p - g_c) & \text{if } U(LBP_{P,R}(g_c)) \le 2 \\ P+1 & \text{otherwise} \end{cases}$$

U- spatial transition

•Number LBP

$$LBP_{P,R}^{num}(g_c) = \begin{cases} \sum_{p=0}^{P-1} s(g_p - g_c) & \text{if } U(LBP_{P,R}(g_c)) \le 2 \\ Num_1\{LBP_{P,R}(g_c)\} & \text{if } \begin{array}{l} U(LBP_{P,R}) > 2 \quad \text{and} \\ Num_1\{LBP_{P,R}(g_c)\} \ge Num_0\{LBP_{P,R}(g_c)\} \end{array} \\ Num_0\{LBP_{P,R}(g_c)\} & \text{if } \begin{array}{l} U(LBP_{P,R}) > 2 \quad \text{and} \\ Num_1\{LBP_{P,R}(g_c)\} < Num_0\{LBP_{P,R}(g_c)\} \end{array} \end{cases}$$

•Median LBP

Num_x – Number of 0 or 1s

$$LBP_{P,R}^{med}(g_c) = \sum_{p=0}^{P-1} s(g_p - \widetilde{g})$$

8

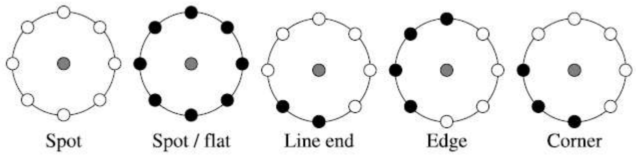

Fig. 2.3 Different texture primitives detected by the LBP

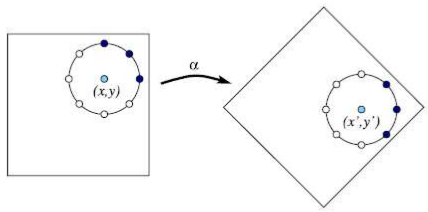

Fig. 2.5 Effect of image rotation on points in circular neighborhoods

9

Midbrain

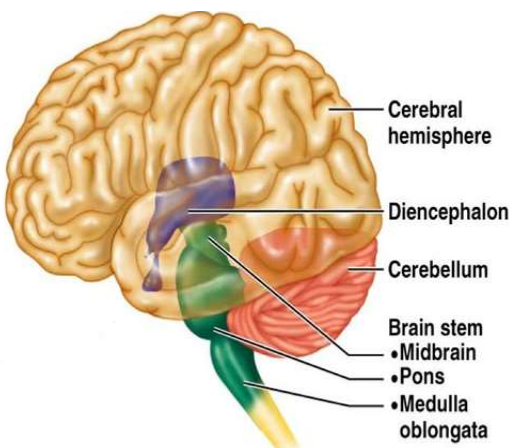

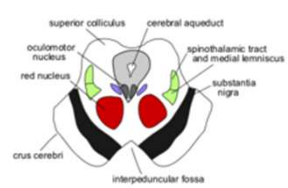

[Wikipedia]

10

Proposal

- A novel method for segmenting midbrain based on the combined use of Active Shape Models (ASM) and Local Binary Patterns (LBP).
  - The joint-model considers both global and local statistics to improve the final shape.
  - Combined use of ASMs to detect midbrain boundaries for strong edges and LBPs improves the segmentation.
  - LBPs add to ASMs the Robustness needed to detect non-salient boundaries in the presence of noise that some other methods lack.
  - Statistical model able to improve structure detection because of the LBPs.

11

Goals

- Improve organ segmentation to quantify medical parameters:
  1. Propose a segmentation model inspired by the human visual system (HVS)
  2. Take advantage the different texture approaches
  3. Evaluate performance of deformable models methods adding texture support.

12

Active Shape Models

- Statistical deformable models
- Detect specific shapes boundaries
- Have a certain variability to ressemble real organ
- Heart [Barba 2012], fetal cerebellum [Becker 210]
- Begin with aligned shapes of an object- Pose transformations

13

Active Shape Models

- Step - Statistical shape PDM

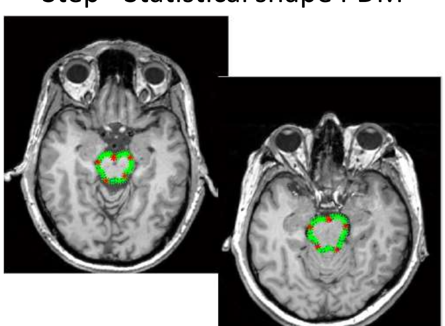

$$S_i = (x_0, y_0, \ldots, x_{n-1}, y_{n-1})^T$$

Principal Component Analysis
(PCA 90-99.5%)

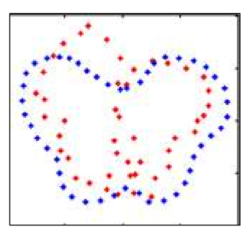

14

Active Shape Models

- Step 1 Gray level models using PDM

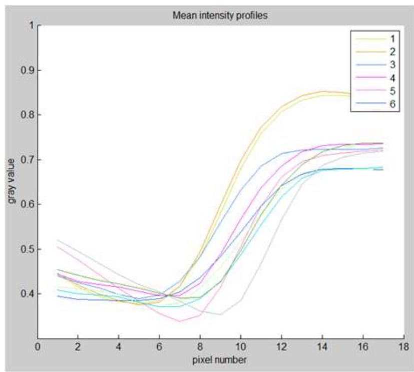

PCA Analysis (90-99.5%)

15

Active Shape Models

•Step 2 ASM search

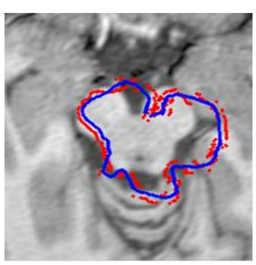

$$\hat{X} = \bar{X} + Pb$$

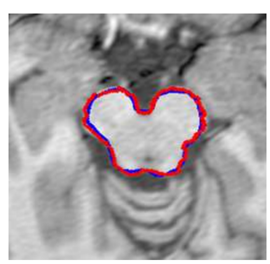

16

Our proposal

- We investigated two different ways to combine both models: LBPs and ASMs.

a) Profile ASM/ LBP histogram for each profile landmark of the contour.

b) Quadratic ASM/LBP histogram for each landmark of the contour. We took 4 regions and concatenated the histograms into a single one.

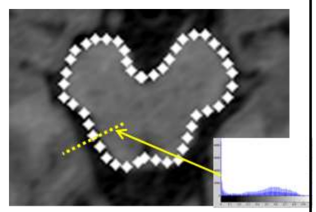

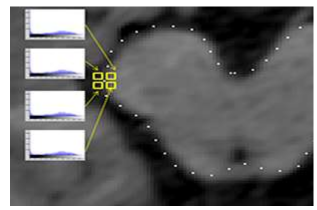

17

ASM2D +LBP Quadratic ASM/LBP

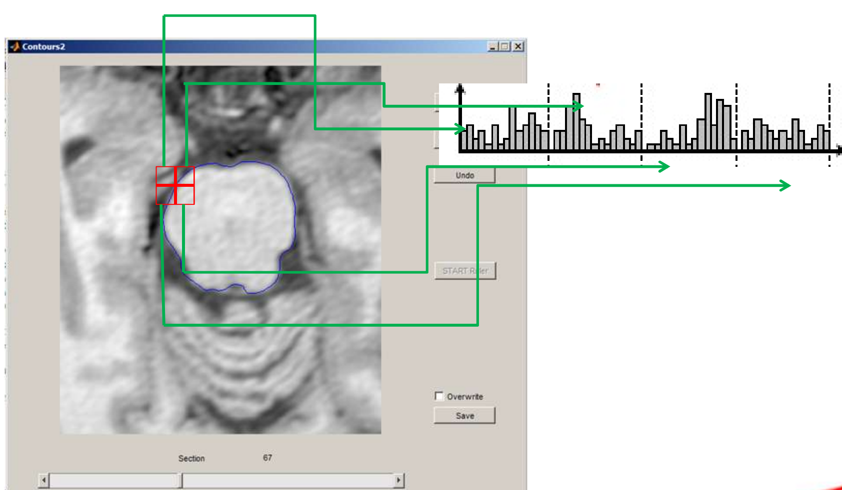

18

Experimental Results

- Dice index $d_D = \frac{2 \times (\|A \cap B\|)}{(\|A\| + \|B\|)}$
  - uses the intersected area between the expert and recognized contours divided by the sum of both areas. The result is a normalized value between 0 and **1**.

- Hausdorff distance $d_H(P, Q) = \max\{d(P, Q), d(Q, P)\}$
  - measures how close a point from a first set is from another point of the second set in a metric space. (**minimum value**)

19

Experimental Results

- ASM only
- Profile ASM/ LBP
  - LBP original
  - LBP Uniform
  - LBP Numeric
  - LBP Median
- Quadratic ASM/LBP
  - LBP original
  - LBP Uniform
  - LBP Numeric
  - LBP Median

20

Experimental Results

Dice index and Hausdorff metric for the ASM algorithm

	ASM	
	Dice	Haussdorf
$\mu\,(\sigma)$	0.6971 ($\pm$0.1730)	17.1229($\pm$8.0789)

	ASM/LBP	ASM/$LBP_{P,R}^{uni}$	ASM/$LBP_{P,R}^{num}$	ASM/$LBP_{P,R}^{med}$
Dice				
$\mu\,(\sigma)$	0.9414($\pm$0.0166)	0.8919($\pm$0.1076)	0.8765($\pm$0.1032)	0.9100($\pm$0.0700)
Haussdorf				
$\mu\,(\sigma)$	5.2968($\pm$1.4303)	7.2765($\pm$4.6658)	9.6498($\pm$7.7566)	7.1582($\pm$4.7602)

21

Experimental Results

Dice index and Hausdorff metric for the ASM algorithm

	ASM	
	Dice	Haussdorf
$\mu\,(\sigma)$	0.6971 ($\pm$0.1730)	17.1229($\pm$8.0789)

	ASM/LBP	ASM/$LBP_{P,R}^{uni}$	ASM/$LBP_{P,R}^{num}$	ASM/$LBP_{P,R}^{med}$
Dice				
$\mu\,(\sigma)$	0.9481($\pm$0.0127)	0.9454($\pm$0.0140)	0.9188($\pm$0.0607)	0.9465($\pm$0.0140)
Haussdorf				
$\mu\,(\sigma)$	4.9359($\pm$1.2626)	4.8195($\pm$1.2956)	6.9448($\pm$4.7815)	5.1174($\pm$1.3755)

22

ASM only

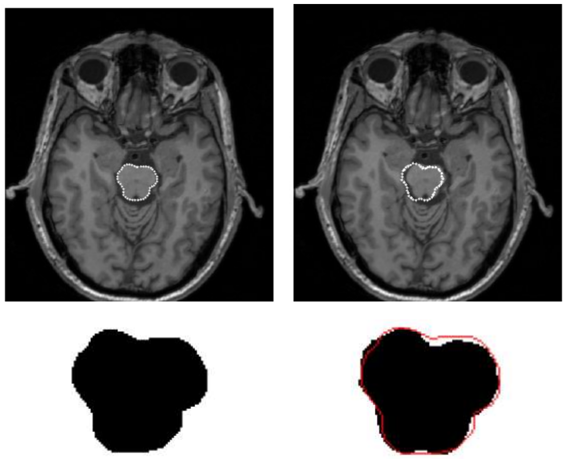

(a) Cranial MR axial view expert annotated

(b) ASM segmented boundary
red contour = expert boundary

23

ASM/LBP Segmentation

Profile:

(a) ASM/LBP

(b) ASM/LBPuni

(c) ASM/LBPnum

(d) ASM/LBPmed

Quadratic:

(a) ASM/LBP

(b) ASM/LBPuni

(c) ASM/LBPnum

(d) ASM/LBPmed

24

Conclusions

•ASM-LBPs offer a better segmentation of midbrain volumes.
• Compare performance of different modalities of ASM/LBP and LBP techniques using midbrain MRI volume images.
•Order of the results:

1) Quadratic LBP algorithm
2) Profile LBP
3) ASM method

•In the case of Profile ASM/LBP scheme the initial position is very important and can vary the results. It could not converge correctly.
•Quadratic ASM/LBP shows a major performance even when we do not have enough data. The reason is the use of a bigger area that characterizes the midbrain contour .

25

Final Result

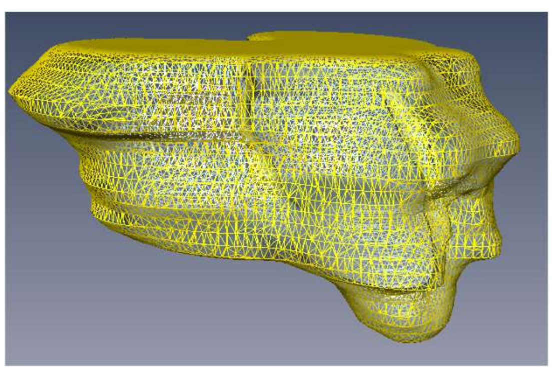

26